

DOI:10.1002/ejic.201300843

# Bimetallic Iridium–Carbene Complexes with Mesoionic Triazolylidene Ligands for Water Oxidation Catalysis

Ana Petronilho,<sup>[a]</sup> James A. Woods,<sup>[b]</sup> Stefan Bernhard,<sup>\*,[b]</sup> and Martin Albrecht<sup>\*,[a]</sup>



*Dedicated to Professor Ernesto Carmona on the occasion of his 65th birthday<sup>[‡]</sup>*

**Keywords:** Water chemistry / Oxidation / Iridium / Carbenes / Bimetallic complexes

Two new diiridium–triazolylidene complexes were prepared as bimetallic analogues of established mononuclear water oxidation catalysts. Both complexes are efficient catalyst precursors in the presence of cerium ammonium nitrate (CAN) as sacrificial oxidant. Up to 20000:1 ratios of CAN/complex, the turnover limitation is the availability of CAN and not the catalyst stability. The water oxidation activity of the bimetallic complexes is not better than the monometallic species at 0.6 mM catalyst concentration. Under dilute conditions

(0.03 mM), the bimetallic complexes double their activity, whereas the monometallic complexes show an opposite trend and display markedly reduced rates, thereby suggesting a benefit of the close proximity of two metal centers in this low concentration regime. The high dependence of catalyst activity on reaction conditions indicates that caution is required when catalysts are compared by their turnover frequencies only.

## Introduction

Artificial photosynthesis is considered a viable and sustainable process for reducing the global dependence on finite fossil-fuel resources.<sup>[1]</sup> A conceivable photosynthetic pathway hence consists of a water reduction cycle (WRC;  $2\text{H}^+ + 2\text{e}^- \rightarrow \text{H}_2$ ) and a concomitant water oxidation cycle (WOC;  $2\text{H}_2\text{O} \rightarrow \text{O}_2 + 4\text{H}^+ + 4\text{e}^-$ ), which results in an overall splitting of water into  $\text{O}_2$  and  $\text{H}_2$  as carbon-neutral fuel.<sup>[2]</sup>

Although stunning performance in catalyst development for the WRC have been achieved,<sup>[3]</sup> WOC is comparably difficult because of the complexity of  $\text{O}_2$  formation and the uphill thermodynamics. Oxygen evolution activity has been demonstrated with a variety of heterogeneous and heterogenized catalysts.<sup>[4]</sup> Recent efforts have furthermore concentrated on molecular catalyst precursors, stimulated by the pioneering work of Meyer et al.<sup>[5]</sup> Conceptually, molecular catalysts offer intriguing benefits such as a well-defined

active site as well as the opportunity to use the structure–activity relationship for tailoring catalytic activity. Indeed, the relevance of the ligand framework has been demonstrated in various studies.<sup>[6]</sup> Appreciable performance was noted with some first-row transition-metal complexes,<sup>[7]</sup> although the most active molecular water oxidation catalysts have emerged thus far from ruthenium and iridium complexes.<sup>[8]</sup> When coordinated to a suitable ligand set, turnover frequencies as high as those of the natural oxygen evolving complex (OEC) have been observed,<sup>[9]</sup> as well as catalyst longevity that enables turnovers in the  $10^4$  range.<sup>[10]</sup> Within this context, triazolylidene ligands,<sup>[11]</sup> a specific class of mesoionic carbenes,<sup>[12]</sup> have recently been shown to impart attractive and tunable properties for water oxidation catalysis.<sup>[10,13]</sup>

The key step in water oxidation catalysis is generally accepted to be the rate-limiting O–O bond formation from the crucial oxidized  $\text{M}=\text{O}$  species.<sup>[14]</sup> Mechanistically, two distinct pathways have been proposed for this step, including either the interaction of two high-valent metal–oxo species ( $\text{M}=\text{O}\cdots\text{O}=\text{M}$  interaction), or the nucleophilic attachment of a water molecule to a metal–oxo site ( $\text{M}=\text{O}\cdots\text{OH}_2$  interaction).<sup>[15]</sup> These different mechanisms have crucial consequences on the ligand and catalyst design, and also on potential catalyst immobilization strategies. A bimetallic mechanism will clearly benefit from a close proximity of the two metal centers (e.g., through intramolecular linkage), whereas the nucleophilic attack will require only one metal

[a] School of Chemistry and Chemical Biology, University College Dublin, Belfield, Dublin 4, Ireland, E-mail: martin.albrecht@ucd.ie  
[www.ucd.ie/chem/staff/profmartinalbrecht/](http://www.ucd.ie/chem/staff/profmartinalbrecht/)

[b] Department of Chemistry, Carnegie Mellon University, 4400 Fifth Avenue, Pittsburgh, PA 15213, USA  
E-mail: bern@cmu.edu  
<http://www.chem.cmu.edu/groups/bernlab/>

[‡] In admiration of his ground-breaking contributions to bond activation and organometallic chemistry in general

site and might become deactivated by the close proximity of another metal center.<sup>[16]</sup> Since direct mechanistic probing of the reaction pathway is extremely challenging due to the multielectron, multiproton transfer involved in water oxidation,<sup>[17]</sup> we set out to synthesize a bimetallic system that might improve the kinetics of water oxidation if an interchange of two M=O units is involved in (rate-limiting) O–O bond formation.<sup>[18]</sup> The known and prolific water oxidation catalyst precursors **1** and **2** provided a valuable starting point for these investigations (Figure 1).<sup>[10,13b]</sup>

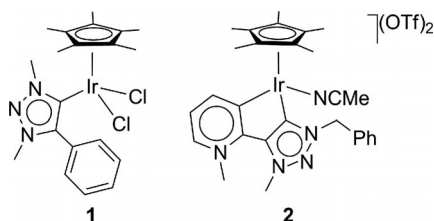
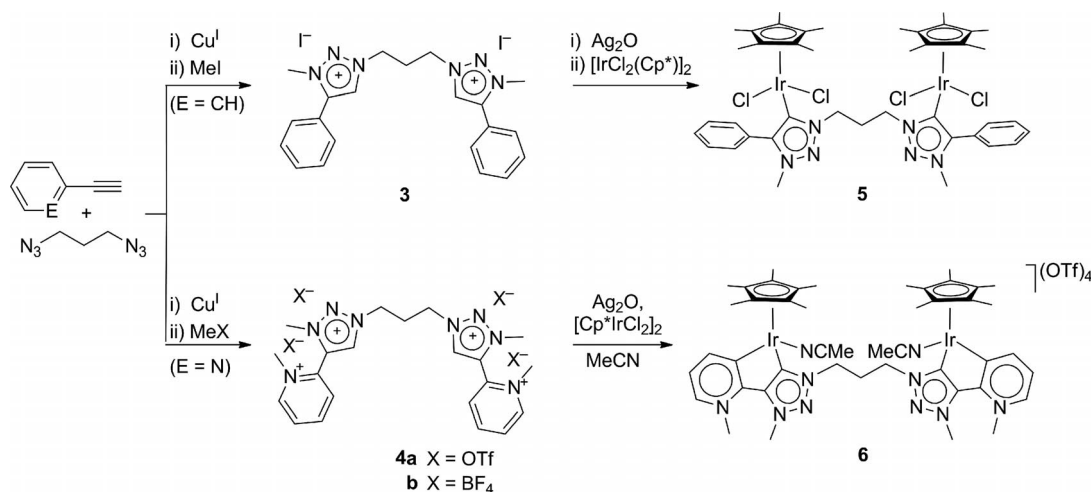


Figure 1. Triazolylidene–iridium complexes **1** and **2** as water oxidation catalyst precursors.

## Results and Discussion

Ditopic ligands that comprise the ligand scaffold of **1** and **2**, respectively, were readily accessible due to the versatility of copper-catalyzed cycloaddition protocols.<sup>[19]</sup> Thus, reaction of diazidopropane with either phenyl or pyridyl acetylene followed by reaction with a methylating agent afforded the desired ligands **3** and **4** in moderate to high yields (Scheme 1). Quaternization of the pyridyl-functionalized di(triazole) intermediate was accomplished both with  $[\text{Me}_3\text{O}]\text{BF}_4$  and with MeOTf, whereas MeI is not reactive enough to install four methyl groups, and methylation occurs only at the pyridine. In contrast, MeI is sufficiently reactive to yield the di(triazolium) salt **3** in high yields (80%).



Scheme 1. Synthesis of complexes **5** and **6**.

In both ligands the trimethylene linker is identified by a characteristic triplet for the  $\text{NCH}_2$  protons around  $\delta_{\text{H}} = 5$  ppm and a quintet for the central  $\text{CH}_2$  group at  $\delta_{\text{H}} = 2.75$  ppm (**3**) or  $\delta_{\text{H}} = 2.95$  ppm (**4**). The acidic triazolium proton appears at low field ( $\delta_{\text{H}} = 9.23$  and 9.25 ppm in **3** and **4**, respectively).

These ligands were metalated according to protocols closely related to those described for the corresponding monometallic complexes **1** and **2**.<sup>[10,13b]</sup> Thus, reaction of di(triazolium) salt **3** with  $\text{Ag}_2\text{O}$  (4 equiv.) for prolonged time at room temperature followed by transmetalation with stoichiometric quantities of  $[\{\text{IrCp}^*\text{Cl}_2\}_2]$  afforded the desired complex **5** (Scheme 1). The bimetallic chelating complex **6** was synthesized by means of a similar transmetalation protocol, although in this case,  $\text{Ag}_2\text{O}$  and the iridium precursor salt were added simultaneously and the metalation was performed at 80 °C. Both complexes are orange, air-stable compounds that dissolve well in MeCN, water, and MeOH. In contrast to the ionic complex **6**, the neutral diiridium complex **5** is also very soluble in chlorinated solvents.

Complexes **5** and **6** share common spectroscopic characteristics. Specifically, the  $\text{Cp}^*/\text{ligand}$  ratio indicates the formation of a bimetallic system rather than a chelating di(triazolylidene) complex. Moreover, the  $\text{NCH}_2$  protons are shifted to higher field. This shift difference is more pronounced in **5** ( $\Delta\delta_{\text{H}} = 1.47$  ppm) than in **6** ( $\Delta\delta_{\text{H}} = 0.24$  ppm). Chelation in **6** is unambiguously deduced from the resonance pattern of the pyridylidene ring, which features two doublets ( $\delta_{\text{H}} = 8.71$  and 8.29 ppm) and a triplet ( $\delta_{\text{H}} = 7.60$  ppm), in agreement with the activation of one  $\text{C}_{\text{py}}\text{--H}$  bond. In **6**, most resonances are broad, and the coupling in the linker is poorly resolved, presumably because of the presence of two diastereoisomers due to the chirality at iridium.<sup>[20]</sup> The presence of two resonances for the  $\text{Cp}\text{--CH}_3$  groups in equal ratio ( $\delta_{\text{H}} = 1.85$  and 1.84 ppm) lends further support to such a model. The iridium-bound carbon resonates at  $\delta_{\text{C}} = 149.7$  ppm in the  $^{13}\text{C}$  NMR spectrum of **5**, and at  $\delta_{\text{C}} = 154.5$  and 153.9 ppm in **6**.

The electrochemical properties of complexes **5** and **6** are unsurprising and do not differ significantly from the monometallic model compounds and from related species.<sup>[21]</sup> For example, complex **6** does not show any distinct redox feature below +1 V (aqueous solution, 1 M HNO<sub>3</sub>, pH = 0) and reveals solvent discharge (i.e., electrocatalytic water oxidation) above this potential.

Both complexes were evaluated as catalysts for the oxidation of water in the presence of sacrificial [Ce(NO<sub>3</sub>)<sub>6</sub>](NH<sub>4</sub>)<sub>2</sub> (CAN) as terminal oxidant. An initial set of experiments was carried out at approximately 0.6 mM concentration of catalyst in a 0.67 M aqueous solution of CAN. Under these conditions, essentially all CAN was consumed within 90 min, and oxygen production was close to the theoretical limit (Figure 2; Table 1, entries 1–4). Inspection of the early stages of the reaction indicates only very minor differences in conversion between the monometallic species **1** and the bimetallic complexes **5** and **6** (inset Figure 2). This similarity is remarkable, because complexes **5** and **6** possess two active metal centers, and hence a higher activity would be expected. Monitoring the rate of oxygen evolution reveals a delicate influence of the ligand scaffold. Thus, the bimetallic complex **5** is significantly slower than the monometallic analogue within the first 1000 s of the reaction (Figure 3, Table 1). The maximum turnover frequency (TOF<sub>max</sub>) of the catalytically active species derived from **1** is about twice as high as that of the bimetallic precursor

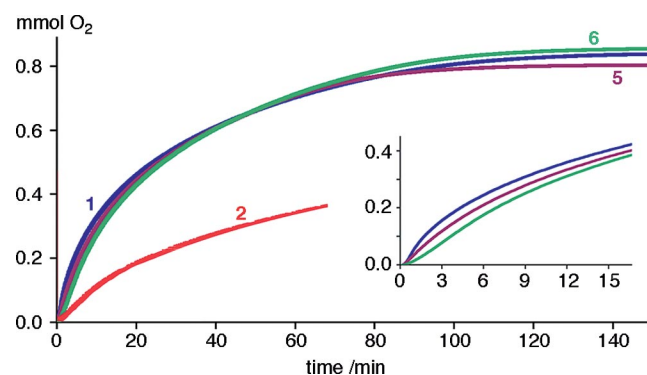


Figure 2. Oxygen evolution with a CAN/complex ratio of approximately 1000:1 (0.6 mM complex) for complexes **1**, **2**, **5**, and **6**. Inset: Oxygen evolution at initial 15 min of the reaction.

Table 1. Catalytic performance of complexes **1**, **5**, and **6**.<sup>[a]</sup>

Entry	Complex [mM]	CAN/complex	TON	TOF <sub>max</sub> [s <sup>-1</sup> ]
1	<b>1</b> (0.65)	1100	260	0.29 (±0.01)
2	<b>2</b> (0.63)	1100	250	0.07 (±0.01)
3	<b>5</b> (0.65)	1100	240	0.17 (±0.03)
4	<b>6</b> (0.69)	1100	230	0.14 (±0.01)
5	<b>1</b> (0.034)	22000	5300	0.22 (±0.05)
6	<b>2</b> (0.035)	22000	5400	0.21 (±0.03)
7	<b>5</b> (0.033)	22000	5500	0.47 (±0.06)
8	<b>6</b> (0.034)	22000	5100	0.29 (±0.02)

[a] Reactions with 0.6 mM complex loading typically performed in 6 mL H<sub>2</sub>O; reactions with 0.03 mM complex in 10 mL H<sub>2</sub>O. Turnover numbers (TONs) calculated at 10000 s and at 48 h, respectively.

(0.29 versus 0.17 s<sup>-1</sup>), which corresponds to some 25% activity of the iridium centers in **5** relative to **1**. The trend is opposite when using the chelating pyridylidene–triazolylidene species **2** and **6** as precursors. The TOF<sub>max</sub> measured from the bimetallic precatalyst is indeed twice as high as that of the monometallic species (0.14 versus 0.07 s<sup>-1</sup>). Maximum rates for **6** were achieved after about 3 min (i.e., at a stage of the reaction when CAN was still in large excess (<10% CAN conversion, namely, CAN/[Ir] ratio >1000:1)). After about 40 min of reaction, the turnover frequencies of **1**, **2**, **5**, and **6** are essentially identical and gradually decrease as CAN is exhausted. This may support a mechanistic model that involves multiple active species with differing levels of catalytic activity as postulated by Beller and co-workers.<sup>[17e]</sup> Accordingly, heterogeneous (and kinetically less competent) species become increasingly prevalent as the reaction proceeds, whereas at initial stages, homogeneously operating catalysts are predominant.

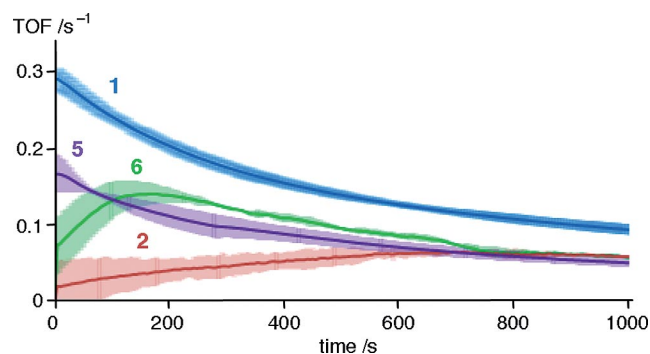


Figure 3. Changes in turnover frequency in water oxidation catalysis with a CAN/complex ratio of approximately 1000:1 (0.6 mM complex) for complexes **1**, **2**, **5**, and **6** over the first 1000 s of O<sub>2</sub> evolution (TOFs measured by manometry with a custom-built transducer setup; see the Experimental Section). Solid lines represent the average of triplicate measurements, faint areas indicates error bands (95% confidence).

A second set of experiments was subsequently performed under more dilute conditions. Lower concentrations are expected to increase the relevance of mononuclear processes (i.e., water nucleophilic attack) in monometallic systems; however, in bimetallic complexes O–O bond formation might still occur through a M=O...O=M interaction due to the locally high concentration of metal centers. Water oxidation with the four iridium complexes **1**, **2**, **5**, and **6** was thus carried out at approximately 0.035 mM catalyst concentration with a CAN/complex ratio of approximately 20000:1 (Table 1, entries 5–8; Figure 4). Oxygen evolution is complete after around 24 h (Figure 4). At this stage, the turnover numbers reached values slightly higher than 5000, thus indicating essentially complete consumption of CAN and efficient conversion of the redox equivalents for O<sub>2</sub> production with all three catalytic systems. The fact that the sacrificial oxidant is turnover-limiting rather than catalyst deactivation suggests that turnover numbers might be markedly increased when using a flow reactor instead of the batch system applied here.

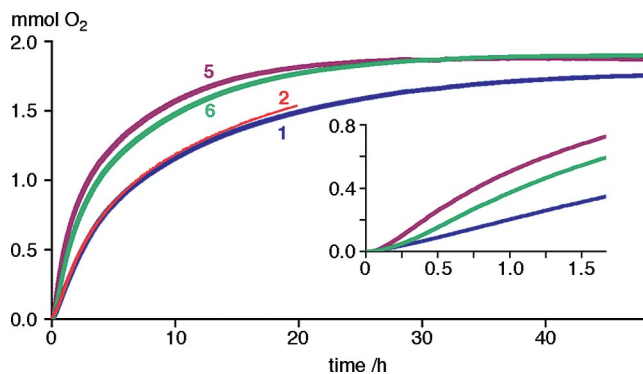


Figure 4. Oxygen evolution with a CAN/complex ratio of approximately 20000:1 (0.03 mM complex) for complexes **1**, **2**, **5**, and **6**. Inset: oxygen evolution at initial 1.5 h of the reaction.

In contrast to the experiments performed at higher catalyst loading, inspection of early stage conversions with low iridium concentrations revealed a significantly higher productivity of the bimetallic complex **5** than the monometallic analogue **1** (inset Figure 4). The different initial reaction rates are illustrated in Figure 5, which indicates a maximum turnover frequency of complex **5** that is now twice as high as that of **1** ( $0.47 \text{ s}^{-1}$  versus  $0.22 \text{ s}^{-1}$ ).<sup>[22]</sup> This behavior is in sharp contrast to the measurements at higher catalyst concentration, whereby the bimetallic species is less efficient (Table 1). These observations might be directly correlated to a potential change in mechanism for these complexes under dilute conditions. Tentatively, the decrease of rate for the monometallic species might be attributed either to a rapid heterogenization (formation of catalytically active colloids) or to an increasing relevance of water nucleophilic attack relative to the interaction of two iridium–oxo species.<sup>[8d]</sup> The opposite effect, namely, the rate increase of the bimetallic complexes under dilute conditions, might speculatively arise from the suppression of undesired intermolecular processes<sup>[16]</sup> that might occur at higher catalyst concentrations, and the preponderance of a mechanism that involves a bimetallic Ir=O...O=Ir interaction in the key step.

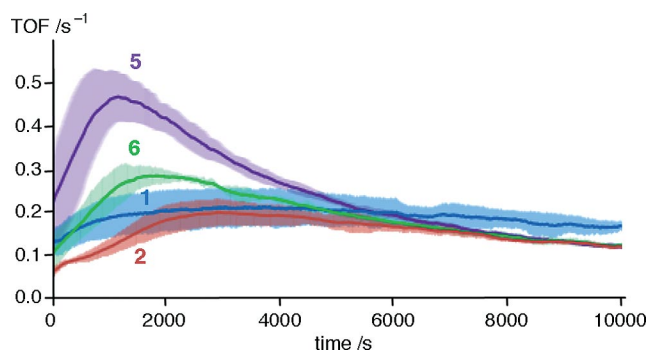


Figure 5. Changes in turnover frequency in water oxidation catalysis with a CAN/complex ratio of approximately 20000:1 (0.03 mM complex) for complexes **1**, **2**, **5**, and **6** over the first 10000 s of O<sub>2</sub> evolution (TOFs measured by manometry). Solid lines represent average of triplicate measurements; faint areas indicate error bands (95% confidence).

With both mono- and bimetallic complexes that contain the bidentate chelating carbene ligand, the maximum turnover rate doubles upon dilution of the catalyst concentration (e.g., from  $0.14 \text{ s}^{-1}$  to  $0.29 \text{ s}^{-1}$  for **6**). Yet, complex **6** is considerably less active than the precatalyst derived from bimetallic **5** with the monodentate bis(carbene) ligand. The lower activity of complex **6** might be attributed to the entropic challenges to reach the appropriate bis(Ir=O) configuration because of the chelating ligand, or indeed to other aspects such as the different partial charge due to the absence or presence of anionic ligands. In any case, the opposite concentration dependence of the rates observed here with mono- and bimetallic systems is remarkable and seems to disfavor a mere complex degradation and formation of colloidal species as the catalytically active species.<sup>[17e,23]</sup> In agreement with this conclusion, headspace analysis of the reaction at different stages by MS did not reveal any CO<sub>2</sub> above the detection threshold (<1 ppm).

## Conclusion

Straightforward synthetic access to bimetallic triazolyliene–iridium complexes has been disclosed. The complexes are active catalyst precursors for CAN-mediated water oxidation. When compared to the monometallic analogues, the activity is improved when water oxidation is performed under dilute catalyst concentrations. This result might point to a change in the mechanism that is related to the concentration of iridium complexes and emphasizes the difficulties associated with using turnover frequencies as the key parameter for the evaluation of catalyst precursors. These results thus strongly underline the relevance of reaction conditions, especially when comparing different catalyst systems. Our results tentatively support a bimetallic O–O bond-forming mechanism at low iridium concentration, although we cannot confidently rule out an oxidative cleavage of the linker, which curtails any benefits from a dimetallic catalyst precursor, especially at higher iridium concentrations, and might lead to a heterogeneous catalyst. Synthetic efforts directed towards installing linkers with different rigidity between the two triazolyliene iridium active sites are currently in progress.

## Experimental Section

**General Comments:** The syntheses of complexes **1**<sup>[13b]</sup> and **2**<sup>[10]</sup> are reported elsewhere. The 1,3-diazidopropane was prepared as described previously<sup>[24]</sup> and was used without isolation as a THF solution (ca. 3 M). All other starting materials and reagents were obtained from commercial sources and were used as received. Microwave reactions were carried out with a Biotage Initiator 2.5 operating at 100 W irradiation power. NMR spectra were recorded with Varian spectrometers operating at 300–600 MHz. Chemical shifts  $\delta$  are reported in ppm ( $J$  in Hz) relative to Me<sub>4</sub>Si or residual protio solvents. Signals were assigned with the aid of two-dimensional cross-coupling experiments. Elemental analysis was per-

formed with an Exeter Analytical CE440 elemental analyzer. High-resolution mass spectrometry was carried out with a Micromass/Waters Corp. USA liquid chromatography time-of-flight spectrometer equipped with an electrospray source.

**Synthesis of 3:** Diazidopropane (3 mL, approx 3 M in THF, 9 mmol) and phenylacetylene (1.5 mL, 16 mmol) were dissolved in a mixture of THF/water (1:1, 15 mL). CuSO<sub>4</sub> (110 mg, 0.70 mmol) and sodium ascorbate (1.4 g, 7 mmol) were added and the mixture was reacted under microwave irradiation at 100 °C for 1 h. The solvents were removed under reduced pressure, and the residue was suspended in CH<sub>2</sub>Cl<sub>2</sub> and washed consecutively with aqueous NH<sub>3</sub> (10%), water, and brine. After drying over MgSO<sub>4</sub> and solvent evaporation, compound **1** was obtained as a white powder 643 mg (25%). The solid was dissolved in MeCN (15 mL) and MeI (1.1 mL, 18 mmol) was added. The mixture was stirred under microwave irradiation at 100 °C for 2 h. Et<sub>2</sub>O was added, and the formed white precipitate was filtered off and dried under vacuum to afford **3** (965 mg, 81%). <sup>1</sup>H NMR (500 MHz, [D<sub>6</sub>]DMSO): δ = 9.25 (s, 2 H; CH<sub>trz</sub>), 7.79–7.75 (m, 4 H; CH<sub>Ph</sub>), 7.71–7.66 (m, 6 H; CH<sub>Ph</sub>), 4.89 (t, <sup>3</sup>J<sub>H,H</sub> = 6.9 Hz, 4 H; NCH<sub>2</sub>), 4.32 (s, NCH<sub>3</sub>), 2.75 (quintet, <sup>3</sup>J<sub>H,H</sub> = 6.9 Hz, 2 H; C–CH<sub>2</sub>–C) ppm. <sup>13</sup>C{<sup>1</sup>H} NMR (125 MHz, [D<sub>6</sub>]DMSO): δ = 142.9 (C<sub>trz</sub>–Ph), 132.0, 129.9, 129.8 (3 × C<sub>Ph</sub>H), 129.7 (C<sub>trz</sub>H), 123.1 (C<sub>Ph</sub>–trz), 50.4 (NCH<sub>2</sub>), 39.4 (NCH<sub>3</sub>), 28.5 (C–CH<sub>2</sub>–C) ppm. HRMS (ES<sup>+</sup>): calcd. for [M – 2I]<sup>2+</sup> 180.1031; found 180.1036. C<sub>21</sub>H<sub>24</sub>I<sub>2</sub>N<sub>6</sub>·0.5H<sub>2</sub>O: calcd. C 40.47, H 4.04, N 13.48; found C 40.38, H 3.74, N 13.11.

**Synthesis of 4:** Diazidopropane (3 mL, approx 3 M in THF, 9 mmol) and 2-ethynylpyridine (1.0 mL, 16 mmol) were dissolved in a THF/water mixture (1:1, 15 mL). CuSO<sub>4</sub> (110 mg, 0.70 mmol) and sodium ascorbate (1.4 g, 7 mmol) were added, and the mixture was reacted under microwave irradiation at 100 °C for 1 h. The solvents were removed under reduced pressure, and the residue was suspended in CH<sub>2</sub>Cl<sub>2</sub> and washed sequentially with aqueous NH<sub>3</sub> (10%), water, and brine. After drying over MgSO<sub>4</sub> and evaporation of all volatiles, the di(triazole) was obtained as a white powder (908 mg, 54%). The triazole (900 mg, 2.7 mmol) was dissolved in a mixture of 1,2-dichloroethane (15 mL) and MeOH (3 mL), and MeOTf (2.5 mL, 23 mmol) was added. After stirring for 48 h at 90 °C, the mixture was cooled to room temp. Addition of Et<sub>2</sub>O yielded a oily residue, which was separated and washed with copious amounts of Et<sub>2</sub>O to give compound **4a** (950 mg, 39%) as a white solid.

Another batch of di(triazole) (430 mg, 1.3 mmol) was dissolved in CH<sub>2</sub>Cl<sub>2</sub> (10 mL), and [Me<sub>3</sub>O]BF<sub>4</sub> (1.3 g, 10 mmol) was added. The mixture was stirred for 36 h, treated with an excess amount of Et<sub>2</sub>O, and the precipitate was added. The mixture was stirred for 36 h, treated with an excess amount of Et<sub>2</sub>O, and the precipitate was isolated and recrystallized from water. The first batch of crystals (79 mg, 12%) yielded analytically pure **4b**. Spectroscopic data for **4a** and **4b** were identical. <sup>1</sup>H NMR (500 MHz, D<sub>2</sub>O): δ = 9.23 (s, 2 H; CH<sub>trz</sub>), 9.18 (d, <sup>3</sup>J<sub>H,H</sub> = 6.1 Hz, 2 H; H<sub>py</sub>), 8.78 (t, <sup>3</sup>J<sub>H,H</sub> = 8.0 Hz, 2 H; H<sub>py</sub>), 8.35–8.31 (m, 4 H; H<sub>py</sub>), 7.70–7.67 (m, 4 H; H<sub>py</sub>), 5.02 (t, <sup>3</sup>J<sub>H,H</sub> = 7.3 Hz, 4 H; NCH<sub>2</sub>), 4.29 (s; NCH<sub>3</sub>), 4.27 (s; NCH<sub>3</sub>), 2.94 (quintet, <sup>3</sup>J<sub>H,H</sub> = 7.3 Hz, 2 H; C–CH<sub>2</sub>–C) ppm. <sup>13</sup>C{<sup>1</sup>H} NMR (125 MHz, D<sub>2</sub>O): δ = 149.7 (C<sub>py</sub>H), 149.7 (C<sub>py</sub>–trz), 147.3 (C<sub>py</sub>H), 133.3 (C<sub>trz</sub>H), 132.8 (C<sub>trz</sub>–py), 132.5 (C<sub>py</sub>H), 131.3 (C<sub>py</sub>H), 51.3 (NCH<sub>2</sub>), 47.5, 39.4 (2 × NCH<sub>3</sub>), 27.3 (C–CH<sub>2</sub>–C) ppm. C<sub>21</sub>H<sub>26</sub>B<sub>4</sub>F<sub>6</sub>N<sub>8</sub> (547.72): calcd. C 34.19, H 3.55, N 15.19; found C 34.23, H 3.42, N 15.19.

**Synthesis of 5:** Compound **3** (100 mg, 0.16 mmol) and Ag<sub>2</sub>O (151 mg, 0.64 mmol) were suspended in dry MeCN (10 mL) and stirred at room temp. for 3 d in the dark. Subsequently,

[[IrCp\*Cl<sub>2</sub>]<sub>2</sub>] (129 mg, 0.16 mmol) was added, and the mixture was stirred for another 24 h. The mixture was filtered through Celite, and the filtrate was evaporated to dryness. The solid residue was dissolved in CH<sub>2</sub>Cl<sub>2</sub>, filtered through Celite, and triturated with Et<sub>2</sub>O to give an orange precipitate, which was isolated and dried under vacuum, yield 70 mg (41%). <sup>1</sup>H NMR (500 MHz, CDCl<sub>3</sub>): δ = 7.65 (d, <sup>3</sup>J<sub>H,H</sub> = 6.4 Hz, 4 H; H<sub>Ar</sub>), 7.41–7.37 (m, 6 H; H<sub>Ar</sub>), 5.00 (br. s, 4 H; NCH<sub>2</sub>), 3.75 (s, 3 H; NCH<sub>3</sub>), 3.0–2.9 (m, 2 H; C–CH<sub>2</sub>–C), 1.36 (s, 30 H; Cp–CH<sub>3</sub>) ppm. <sup>13</sup>C{<sup>1</sup>H} NMR (125 MHz, CDCl<sub>3</sub>): δ = 149.7 (C<sub>trz</sub>–Ir), 132.6, 129.7, 127.8 (3 × C<sub>Ph</sub>H), 127.8 (C<sub>trz</sub>–Ph), 127.7 (C<sub>Ph</sub>–trz), 88.1 (C<sub>Cp</sub>–Me), 50.6 (NCH<sub>2</sub>), 37.3 (NCH<sub>3</sub>), 31.5 (br., C–CH<sub>2</sub>–C), 9.0 (CH<sub>3</sub>–Cp) ppm. HRMS (ES<sup>+</sup>): calcd. for [M + Na]<sup>+</sup> 1177.2200; found 1177.2164. C<sub>41</sub>H<sub>52</sub>Cl<sub>4</sub>Ir<sub>2</sub>N<sub>6</sub> (1155.15): calcd. C 42.63, H 4.54, N 7.28; found C 42.78, H 4.26, N 6.45.<sup>[25]</sup>

**Synthesis of 6:** Compound **4a** (100 mg, 0.15 mmol), [[IrCp\*Cl<sub>2</sub>]<sub>2</sub>] (115 mg, 0.15 mmol) and Ag<sub>2</sub>O (100 mg, 0.43 mmol) were suspended in dry MeCN (10 mL) and stirred at 80 °C for 24 h in the absence of light. After cooling to room temp., the reaction mixture was filtered through Celite and Et<sub>2</sub>O was added, which induced the formation of an orange precipitate. This precipitate was dissolved in MeOH, filtered, and layered with Et<sub>2</sub>O, which induced slow formation of an orange precipitate. Further precipitation was accomplished upon storing the mixture at –23 °C for 2 h. The precipitate was collected and dried under vacuum, yield 79 mg (36%). <sup>1</sup>H NMR (400 MHz, CD<sub>3</sub>CN): δ = 8.71 (d, <sup>3</sup>J<sub>H,H</sub> = 7 Hz, 2 H; H<sub>py</sub>), 8.29 (d, <sup>3</sup>J<sub>H,H</sub> = 7 Hz, 2 H; H<sub>py</sub>), 7.60 (t, <sup>3</sup>J<sub>H,H</sub> = 7 Hz, 1 H; H<sub>py</sub>), 4.9–4.6 (m, 4 H; NCH<sub>2</sub>), 4.61, 4.58 (2 × s, 3 H; NCH<sub>3</sub>), 2.75–2.65 (m, 2 H; C–CH<sub>2</sub>–C), 1.85, 1.84 (2 × s, 15 H; Cp–CH<sub>3</sub>) ppm. <sup>13</sup>C{<sup>1</sup>H} NMR (100 MHz, CD<sub>3</sub>CN): δ = 155.2 (C<sub>py</sub>–trz), 154.5 (C<sub>trz</sub>–Ir), 153.9 (C<sub>py</sub>–Ir), 152.5 (C<sub>py</sub>H), 149.2 (C<sub>trz</sub>–py), 140.0, 125.2 (2 × C<sub>py</sub>H), 94.4 (C<sub>Cp</sub>–Me), 50.9 (NCH<sub>2</sub>), 44.7, 44.2 (2 × NCH<sub>3</sub>), 29.5 (C–CH<sub>2</sub>–C), 8.8 (CH<sub>3</sub>–Cp) ppm. HR-MS (ES<sup>+</sup>): calcd. for C<sub>42</sub>H<sub>50</sub>F<sub>6</sub>Ir<sub>2</sub>N<sub>9</sub>O<sub>6</sub>S<sub>2</sub> [M – 2MeOTf, CH<sub>3</sub>]<sup>2+</sup> 670.1244; found 670.1313. C<sub>49</sub>H<sub>60</sub>F<sub>12</sub>Ir<sub>2</sub>N<sub>10</sub>O<sub>12</sub>S<sub>4</sub> (1721.73): calcd. C 34.18, H 3.51, N 8.14; found C 34.10, H 3.38, N 7.31.<sup>[25]</sup>

**Catalytic Water Oxidation:** For measurements at higher concentration, a solution of the indicated catalyst (1 mL; see Table 1 for final catalyst concentrations) was added to a sealed vial that contained CAN (5 mL, 0.8 M, 4.0 mmol). Experiments under dilute conditions were performed by adding the indicated catalyst (0.1 mL) to a sealed vial that contained CAN (10 mL, 0.8 M, 8.0 mmol). For both sets of experiments, the resulting pressure increase was monitored by means of manometry. End points were verified by gas chromatography and corrected for nitrogen contamination. Head-space MS analysis was performed at different stages of the reaction. Further experimental details are reported in the literature.<sup>[6a]</sup>

## Acknowledgments

This work has been financially supported by the European Research Council (ERC StG 208651, ERC PoC 324609), and by the Science Foundation Ireland (Solar Research Cluster). S. B. gratefully acknowledges support by the National Science Foundation (CHE-1055547). We thank Johnson Matthey for a generous loan of iridium.

[1] a) N. D. McDaniel, S. Bernhard, *Dalton Trans.* **2010**, 39, 10021–10030; b) C. Herrero, A. Quaranta, W. Leibl, A. W. Rutherford, A. Aukauloo, *Energy Environ. Sci.* **2011**, 4, 2353–

- 2365; c) K. J. Young, L. A. Martini, R. L. Milot, R. C. Snoeberger, V. S. Batista, C. A. Schmuttenmaer, R. H. Crabtree, G. W. Brudvig, *Coord. Chem. Rev.* **2012**, *256*, 2503–2520; d) N. S. Lewis, D. G. Nocera, *Proc. Natl. Acad. Sci. USA* **2006**, *103*, 15729–15735; e) W. Ruttiger, G. C. Dismukes, *Chem. Rev.* **1997**, *97*, 1–24; f) J. J. Concepcion, R. L. House, J. M. Papanikolas, T. J. Meyer, *Proc. Natl. Acad. Sci. USA* **2012**, *109*, 15560–15564.
- [2] S. Y. Reece, J. A. Hamel, K. Sung, T. D. Jarvi, A. J. Esswein, J. J. H. Pijpers, D. G. Nocera, *Science* **2011**, *334*, 645–648.
- [3] Z. Han, F. Qiu, R. Eisenberg, P. L. Holland, T. D. Krauss, *Science* **2012**, *338*, 1321–1324.
- [4] a) M. W. Kanan, D. G. Nocera, *Science* **2008**, *321*, 107; b) W. J. Youngblood, S. H.-A. Lee, K. Maeda, T. E. Mallouk, *Acc. Chem. Res.* **2009**, *42*, 1966–1973; c) Y. Surendranath, M. Dinca, D. G. Nocera, *J. Am. Chem. Soc.* **2009**, *131*, 2615–2620; d) E. M. P. Steinmiller, K. S. Choi, *Proc. Natl. Acad. Sci. USA* **2009**, *106*, 20633–20636; e) M. Dinca, Y. Surendranath, D. G. Nocera, *Proc. Natl. Acad. Sci. USA* **2010**, *107*, 10337–10341; f) S. D. Tilley, M. Cornuz, K. Sivula, M. Grätzel, *Angew. Chem.* **2010**, *122*, 6549; *Angew. Chem. Int. Ed.* **2010**, *49*, 6405–6408; g) N. H. Chou, P. N. Ross, A. T. Bell, T. D. Tilley, *ChemSusChem* **2011**, *4*, 1566–1569; h) R. D. L. Smith, M. S. Prevot, R. D. Fagan, Z. Zhang, P. A. Sedach, M. K. J. Siu, S. Trudel, C. P. Berlinguette, *Science* **2013**, *340*, 60–63.
- [5] a) B. A. Moyer, T. J. Meyer, *J. Am. Chem. Soc.* **1978**, *100*, 3601–3603; b) J. A. Gilbert, D. S. Eggleston, W. R. Murphy, D. A. Geselowitz, S. W. Gersten, D. J. Hodgson, T. J. Meyer, *J. Am. Chem. Soc.* **1985**, *107*, 3855–3864.
- [6] a) N. D. McDaniel, F. J. Coughlin, L. L. Tinker, S. Bernhard, *J. Am. Chem. Soc.* **2008**, *130*, 210–217; b) J. D. Blakemore, N. D. Schley, D. Balcells, J. F. Hull, G. W. Olack, C. D. Incarvito, O. Eisenstein, G. W. Brudvig, R. H. Crabtree, *J. Am. Chem. Soc.* **2010**, *132*, 16017–29; c) J. DePasquale, I. Nieto, L. E. Reuther, C. J. Herbst-Gervasoni, J. J. Paul, V. Mochalin, M. Zeller, C. M. Thomas, A. W. Addison, Elizabeth T. Papish, *Inorg. Chem.* **2013**, *52*, (DOI: 10.1021/ic302448d).
- [7] a) J. Limburg, J. S. Vrettos, L. M. Liable-Sands, A. L. Rheingold, R. H. Crabtree, G. W. Brudwig, *Science* **1999**, *283*, 1524–1527; b) W. C. Ellis, N. D. McDaniel, S. Bernhard, T. J. Collins, *J. Am. Chem. Soc.* **2010**, *132*, 10990–10991; c) J. L. Fillol, Z. Codola, I. Garcia-Bosch, L. Gomez, J. J. Pla, M. Costas, *Nat. Chem.* **2011**, *3*, 807–813; d) S. M. Barnett, K. I. Goldberg, J. M. Mayer, *Nat. Chem.* **2012**, *4*, 498–502; e) P. Du, R. Eisenberg, *Energy Environ. Sci.* **2012**, *5*, 6012–6021.
- [8] a) I. Romero, M. Rodriguez, C. Sens, J. Mola, M. R. Kollipara, L. Francas, E. Mas-Marza, L. Escriche, A. Llobet, *Inorg. Chem.* **2008**, *47*, 1824–1834; b) X. Sala, M. Rodriguez, I. Romero, L. Escriche, A. Llobet, *Angew. Chem.* **2009**, *121*, 2882; *Angew. Chem. Int. Ed.* **2009**, *48*, 2842–2852; c) J. J. Concepcion, J. W. Jurss, M. K. Brennaman, P. G. Hoertz, A. O. T. Patrocinio, N. Y. M. Iha, J. L. Templeton, T. J. Meyer, *Acc. Chem. Res.* **2009**, *42*, 1954–1965; d) S. Romain, L. Vigara, A. Llobet, *Acc. Chem. Res.* **2009**, *42*, 1944–1953; e) H. Yamazaki, A. Shouji, M. Kajita, M. Yagi, *Coord. Chem. Rev.* **2010**, *254*, 2483–2491; f) F. Puntoriero, A. Sartorel, M. Orlandi, G. La Ganga, S. Serroni, M. Bonchio, F. Scandola, S. Campagna, *Coord. Chem. Rev.* **2011**, *255*, 2594–2601; g) A. Sartorel, M. Bonchio, S. Campagna, F. Scandola, *Chem. Soc. Rev.* **2013**, *42*, 2262–2280; h) D. G. H. Hetterscheid, J. I. van der Vlugt, B. de Bruin, J. N. H. Reek, *Angew. Chem.* **2012**, *51*, 9740–9747.
- [9] L. Duan, F. Bozoglian, S. Mandal, B. Stewart, T. Privalov, A. Llobet, L. Sun, *Nat. Chem.* **2012**, *4*, 418–423.
- [10] R. Lalrempuia, N. D. McDaniel, H. Müller-Bunz, S. Bernhard, M. Albrecht, *Angew. Chem.* **2010**, *122*, 9959; *Angew. Chem. Int. Ed.* **2010**, *49*, 9765–9768.
- [11] a) P. Mathew, A. Neels, M. Albrecht, *J. Am. Chem. Soc.* **2008**, *130*, 13534–13535; b) G. Guisado-Barrios, J. Bouffard, B. Donnadieu, G. Bertrand, *Angew. Chem.* **2010**, *122*, 4869; *Angew. Chem. Int. Ed.* **2010**, *49*, 4759–4762; c) K. F. Donnelly, A. Pe-tronilho, M. Albrecht, *Chem. Commun.* **2013**, *49*, 1145–1159; d) J. D. Crowley, A.-L. Lee, K. J. Kilpin, *Aust. J. Chem.* **2011**, *64*, 1118–1132.
- [12] a) O. Schuster, L. Yang, H. G. Raubenheimer, M. Albrecht, *Chem. Rev.* **2009**, *109*, 3445–3478; b) M. Albrecht, *Chem. Commun.* **2008**, 3601–3610.
- [13] a) L. Bernet, R. Lalrempuia, W. Ghattas, H. Mueller-Bunz, L. Vigara, A. Llobet, M. Albrecht, *Chem. Commun.* **2011**, *47*, 8058–8060; b) A. Petronilho, M. Rahman, J. A. Woods, H. Al-Sayyed, H. Mueller-Bunz, J. M. D. MacElroy, S. Bernhard, M. Albrecht, *Dalton Trans.* **2012**, *41*, 13074–13080.
- [14] a) M. H. V. Huynh, T. J. Meyer, *Chem. Rev.* **2007**, *107*, 5004–5064; b) J. M. Mayer, *Acc. Chem. Res.* **2011**, *44*, 36–46; c) Z. Chen, J. J. Concepcion, X. Hu, W. Yang, P. G. Hoertz, T. J. Meyer, *Proc. Natl. Acad. Sci. USA* **2010**, *107*, 7225–7229; d) L. Vilella, P. Vidossich, D. Balcells, A. Lledos, *Dalton Trans.* **2011**, *40*, 11241–11247; e) S. Gosh, M.-H. Baik, *Angew. Chem.* **2012**, *124*, 1247; *Angew. Chem. Int. Ed.* **2012**, *51*, 1221–1224; f) X. Lin, X. Hu, J. J. Concepcion, Z. Chen, S. Liu, T. J. Meyer, W. Yang, *Proc. Natl. Acad. Sci. USA* **2012**, *109*, 15669–15672.
- [15] S. Romain, L. Vigara, A. Llobet, *Acc. Chem. Res.* **2009**, *42*, 1944–1953.
- [16] a) A. Llobet, M. E. Curry, H. T. Evans, T. J. Meyer, *Inorg. Chem.* **1989**, *28*, 3131–3137; b) C. Sens, I. Romero, M. Rodriguez, A. Llobet, T. Parella, J. Benet-Buchholz, *J. Am. Chem. Soc.* **2004**, *126*, 7798–7799; c) T. B. Brewster, J. D. Blakemore, N. D. Schley, C. D. Incarvito, N. Hazari, G. W. Brudvig, R. H. Crabtree, *Organometallics* **2011**, *30*, 965–973.
- [17] a) N. D. Schley, J. D. Blakemore, N. K. Subbaiyan, C. D. Incarvito, F. D'Souza, R. H. Crabtree, G. W. Brudvig, *J. Am. Chem. Soc.* **2011**, *133*, 10473–10481; b) A. Savini, G. Bellachima, G. Ciancaleoni, C. Zuccaccia, D. Zuccaccia, A. Macchioni, *Chem. Commun.* **2010**, *46*, 9218–9219; c) C. Zuccaccia, G. Bellachima, S. Bolaño, L. Rocchigiani, A. Savini, A. Macchioni, *Eur. J. Inorg. Chem.* **2012**, 1462–1468; d) C. Wang, J.-L. Wang, W. Lin, *J. Am. Chem. Soc.* **2012**, *134*, 19895–19908; e) H. Junge, N. Marquet, A. Kammer, S. Denurra, M. Bauer, S. Wohlrab, F. Gärtner, M.-M. Pohl, A. Spannenberg, S. Gladiali, M. Beller, *Chem. Eur. J.* **2012**, *18*, 12749–12758; f) U. Hintermair, S. M. Hashmi, M. Elimelech, R. H. Crabtree, *J. Am. Chem. Soc.* **2012**, *134*, 9785–9795.
- [18] For examples using a related approach involving bimetallic ruthenium complexes, see: a) R. Zong, R. P. Thummel, *J. Am. Chem. Soc.* **2005**, *127*, 12802–12803; b) Y. Xu, T. Åkermark, V. Gyollai, D. Zou, L. Eriksson, L. Duan, R. Zhang, B. Åkermark, L. Sun, *Inorg. Chem.* **2009**, *48*, 2717–2719; c) Y. Xu, A. Fischer, L. Duan, L. Tong, E. Gabrielsson, B. Åkermark, L. Sun, *Angew. Chem.* **2010**, *122*, 9118; *Angew. Chem. Int. Ed.* **2010**, *49*, 8934–8937; d) J. Mola, C. Dinoi, X. Sala, M. Rodriguez, I. Romero, T. Parella, X. Fontrodona, A. Llobet, *Dalton Trans.* **2011**, *40*, 3640–3646; e) J. Garcia-Anton, R. Bofill, L. Escriche, A. Llobet, X. Sala, *Eur. J. Inorg. Chem.* **2012**, 4775–4789; f) N. Kaveevivitchai, R. Chitta, R. Zong, M. El Ojaimi, R. P. Thummel, *J. Am. Chem. Soc.* **2012**, *134*, 10721–10724; g) Y. Jiang, F. Li, B. Zhang, X. Li, X. Wang, F. Huang, L. Sun, *Angew. Chem. Int. Ed.* **2013**, *52*, 3398–3401. For polynuclear systems, see: h) A. Sartorel, M. Bonchio, S. Campagna, F. Scandola, *Chem. Soc. Rev.* **2013**, *42*, 2262–2280.
- [19] a) R. Huisgen, *Angew. Chem.* **1963**, *75*, 604; *Angew. Chem. Int. Ed. Engl.* **1963**, *2*, 565–598; b) H. Kolb, M. G. Finn, K. B. Sharpless, *Angew. Chem.* **2001**, *113*, 2056; *Angew. Chem. Int. Ed.* **2001**, *40*, 2004–2021.
- [20] a) J. A. Mata, A. R. Chianese, J. R. Miecznikowski, M. Poyatos, E. Peris, J. W. Faller, R. H. Crabtree, *Organometallics* **2004**, *23*, 1253–1263; b) L. Mercs, A. Neels, H. Stoeckli-Evans, M. Albrecht, *Dalton Trans.* **2009**, 7168–7178.
- [21] A. Bucci, A. Savini, L. Rocchigiani, C. Zuccaccia, S. Rizzato, A. Albinati, A. Llobet, A. Macchioni, *Organometallics* **2012**, *31*, 8071–8074.

- [22] Turnover frequencies for all complexes were highest within the first 10–30 min of the catalytic experiments [i.e., at a stage when conversions were less than 10% and CAN was present in a large excess amount (ca. 18000:1 CAN/[Ir])]. At this stage, therefore,  $d[\text{CAN}]/dt$  is approximately zero.
- [23] a) J. D. Blakemore, N. D. Schley, M. N. Kushner-Lenhoff, A. M. Winter, F. D'Souza, R. H. Crabtree, G. W. Brudvig, *Inorg. Chem.* **2012**, *51*, 7749–7763; b) R. H. Crabtree, *Chem. Rev.* **2012**, *112*, 1536–1554.
- [24] a) J. J. Blumenstein, C. J. Michejda, *Tetrahedron Lett.* **1991**, *32*, 183–186; b) S. G. Alvarez, M. T. Alvarez, *Synthesis* **1997**, *4*, 413–414.
- [25] Multiple elemental analyses of several different recrystallized batches of complexes **5** and **6** consistently revealed correct C/H values but N percentages that were too low. Potentially, the bimetallic samples might form barely combustible iridium nitride fractions that lower the measured fraction of  $\text{N}_2$ .

Received: July 3, 2013

Published Online: August 30, 2013